Involvement of Impaired Angiogenesis and Myelosuppression in Antiresorptive-agent Related Osteonecrosis of the Jaw Mouse Model

Hisao IGARASHI[*1], Satoru NISHIZAWA[*2], Takeshi MIYAMOTO[*3], Atsuhiko HIKITA[*4] and Kazuto HOSHI[*1, 4, 5]

[*1]*Department of Sensory and Motor System Medicine, Department of Oral and Maxillofacial Surgery, Dentistry and Orthodontics, The University of Tokyo Graduate School of Medicine*
[*2]*Translational Research Center, The University of Tokyo Hospital*
[*3]*Department of Orthopaedic Surgery, Kumamoto University*
[*4]*Division of Tissue Engineering, The University of Tokyo Hospital*
[*5]*Department of Oral-maxillofacial Surgery, Dentistry and Orthodontics, The University of Tokyo Hospital*

(Received November 29, 2022; Accepted December 8, 2022)

Objective: To explore the involvement of bone marrow cells and angiogenesis in the pathogenesis of antiresorptive agent-related osteonecrosis of the jaw (ARONJ).
Methods: We performed micro-computed tomography (CT) and histological analyses in an ARONJ mouse model generated using bisphosphonate (BP) and cyclophosphamide (CY).
Results: Micro-CT analysis showed that BP and CY inhibited osteoneogenesis in the extraction socket. Histological analysis at 3 days after tooth extraction showed inhibition of vascular endothelial cell and mesenchymal stem cell mobilization into the extraction socket. When neovascularization of the extraction fossa was observed from as early as 1 day after extraction, it occurred predominantly in the area adjacent to the extraction fossa and close to the bone marrow cavity. In addition, the extraction fossa communicated with the adjacent bone marrow via the vasculature. Histological evaluation of the alveolar bone marrow around the extraction socket showed a decrease in bone marrow cells in the BP + CY group.
Conclusion: Both inhibition of angiogenesis and suppression of bone marrow cell mobilization are involved in the pathogenesis of ARONJ.

Key words: ARONJ, bisphosphonate, cyclophosphamide, bone marrow, angiogenesis

INTRODUCTION

First reported by Marx in 2003, bisphosphonate (BP)-related osteonecrosis of the jaw, which is now known as antiresorptive agent-related osteonecrosis of the jaw (ARONJ), is a severe side effect of antiresorptive therapy [1–3]. ARONJ is resistant to therapy and results in marked impairment of activities of daily living because of oral feeding disorder, pain, and infection [4, 5]. There are several known risk factors for ARONJ that can result in serious infection and bone necrosis, including periodontitis, poor oral hygiene, cancer treatment, and tooth extraction [6–8]. Although conservative treatments have been reported for ARONJ, they are not always effective in the advanced stages [3]. On the other hand, surgical treatments such as marginal or segmental resection of the jaw have been reported as viable options with high success rates for all stages of the disease [9, 10]. Basic studies regarding treatment of ARONJ have reported the potential efficacy of disturbance of HMGB1/RAGE signaling [11], administration of inactive N-BP [12], geranylgeraniol (GGOH) [13, 14], tetrahedral framework nucleic acid carrying angiogenic peptide [15], and hyperbaric oxygen therapy [16], although these treatments have not yet been shown to be effective in clinical settings. Although the precise mechanism underlying the pathogenesis of ARONJ is still unclear, the suppression of bone remodeling caused by disturbance of osteoclast activation [17] by BPs is thought to be one of the causes of osteonecrosis of the jaw. Recent studies suggest that ARONJ is related to BP-induced activation of M1 macrophages via TLR-4 [18], facilitation of osteoclast ferroptosis by ubiquitination or degradation of p53 via FBXO9 [19], and the involvement of chromosome 8 locus [20], although these findings cannot fully explain the pathogenesis of the disease [21, 22]. In addition, the specific mechanism by which healing is impaired is unknown, and it is not yet clear which cells are mobilized and involved in healing the scar after tooth extraction. Neovascularization has been reported to be an important factor in the pathogenesis of ARONJ [23, 12]. A recent study reported that osteogenesis of extraction sockets and osteointegration of dental implants involve nearby bone marrow-derived cells expressing Gli-1 [24]. Computed tomography (CT) and magnetic resonance imaging (MRI) studies of MRONJ patients with decreased jaw bone marrow space and other changes have suggested that changes in the bone marrow may be involved in the pathogenesis of

Kazuto HOSHI, Department of Oral-maxillofacial Surgery, Dentistry and Orthodontics, The University of Tokyo Hospital, 7-3-1 Hongo Bunkyo-ku, Tokyo 113-8655, Japan Tel: +81-3-3815-5411 Fax: +81-3-3817-0798 E-mail: HOSHI-ORA@h.u-tokyo.ac.jp

ARONJ [25, 26], but this issue has not been analyzed in detail. In this study, we examined the changes in bone marrow and blood vessels in a mouse model of ARONJ to examine their involvement in the pathogenesis of ARONJ.

MATERIALS AND METHODS

Animals

Sixty C57BL/6J mice (female, 6 weeks old; CLEA Japan, Inc., Tokyo, Japan) were randomly assigned to each treatment group ($n = 5$ per group) to assess the effects of subcutaneous (s.c.) administration of the BP zoledronic acid (Zometa®; Novartis International AG, Basel, Switzerland) prior to tooth extraction with or without intraperitoneal (i.p.) administration of cyclophosphamide (CY) (Shionogi & Co., Ltd., Osaka, Japan). The treatment groups were as follows: tooth extraction (Extraction); tooth extraction post-BP administration (Extraction + BP); and tooth extraction post-BP + CY administration (Extraction + BP + CY). All animal experiments were performed in accordance with the ethical guidelines of the University of Tokyo (ethics approval numbers: H19−198). The investigation conformed to *The Guide for the Care and Use of Laboratory Animals* published by the U.S. National Institutes of Health (NIH Publication No. 85−23, revised 1996).

Induction of the ARONJ Mouse Model

The ARONJ mouse model was induced as described previously [27, 28]. Briefly, BP and/or CY (150 mg/kg twice a week, i.p.) were administered 3 weeks prior to tooth extraction. Mice were anesthetized with a mixture of medetomidine hydrochloride (Domitor; Kyoritsu Seiyaku Corp., Tokyo, Japan), midazolam (Sandoz K.K., Tokyo, Japan), and butorphanol (Meiji Animal Health Co., Kumamoto, Japan) [29], and the maxillary first molar on the left side was extracted under a microscope. After extraction, BP (0.05 mg/kg twice a week, s.c.) and/or CY (150 mg/kg once a week, i.p.) were administered. The maxilla was harvested en bloc at 1, 3, 7, or 14 days after tooth extraction. Untreated mice who had a tooth extracted (Extraction) were used as controls.

Macroscopic Photography of Tooth Extraction Sites

Macroscopic photographs of tooth extraction sites were taken 0, 1, 3, 7, and 14 days after extraction using Leica S9D and MC170HD (Leica, Wetzlar, Germany). Macroscopic images were evaluated with ImageJ 1.49 (National Institutes of Health, Bethesda, MD, USA) to calculate the open wound area [30].

Micro-CT of Tooth Extraction Sites

Harvested maxillae fixed overnight in 4% paraformaldehyde (Fujifilm Wako Pure Chemical Corp., Osaka, Japan) were analyzed via micro-CT imaging before decalcification. Micro-CT analysis was performed using a scanner at 70 kV and 130 mA (InspeXio; Shimadzu Science East Corp., Tokyo, Japan). Three-dimensional (3D) images were reconstructed with TRI/3D-BON (Ratoc Systems, Osaka, Japan). Total volume (TV), bone volume (BV), and bone mineral density (BMD) of ectopically mineralized components in extraction sites were calculated.

Histological Examination of Tooth Extraction Sites and Bone Marrow Cavities

Harvested maxillae were fixed overnight in 4% paraformaldehyde, and decalcified for 4 weeks with 10% EDTA (Dojindo Laboratories Co., Ltd., Kumamoto, Japan), which was replaced twice a week. After decalcification, the samples were embedded in paraffin and cut into coronal sections at the mesial side of the extraction site (5 μm thick) using a microtome (RM2265; Leica). Sections were stained with hematoxylin & eosin (H&E) (Sakura Finetek Japan Co., Ltd., Tokyo, Japan), tartrate-resistant acid phosphatase (TRAP) (Fujifilm Wako Pure Chemical Corp.), Masson's trichrome (Muto Pure Chemicals Co., Ltd., Tokyo, Japan) and picro-sirius red (Muto Pure Chemicals). They were also immunostained with antibodies against CD31 (1 : 100; Abcam, Cambridge, MA, USA), periostin (1 : 100; Abcam), or leptin receptor (1 : 2000; R&D Systems, Minneapolis, MN, USA). Then, secondary antibodies were applied, and the sections were washed three times for 2 min each time. The sections were developed in diaminobenzidine (DAB) (Vector Laboratories, Burlingame, CA, USA). Images were taken under an optical microscope (DP 70; Olympus, Tokyo, Japan). The percentage of empty lacunae, vascularization, and the shape of bone marrow cells in H&E-stained specimens were calculated using ImageJ 1.49 (National Institutes of Health).

Statistical analysis

Statistical analyses were performed using EZR software (Saitama Medical Center, Hidaka, Japan) [31]. The results are expressed as the mean ± standard deviation (SD). The *t* test or Mann-Whitney U test were used for comparison of two variables, and differences among groups were analyzed by one-way analysis of variance (ANOVA) followed by a *post hoc* Tukey test. In all analyses, $P < 0.05$ was taken to indicate statistical significance.

RESULTS

Inhibition of Oral Mucosal Healing in the ARONJ Model

Figure 1A shows the time course for the creation of the ARONJ mouse model. We first evaluated the effects of BP and CY on mucosal healing after tooth extraction. In the Extraction (control) group, the oral mucosa of the extraction socket showed bleeding immediately after extraction, granulation on day 1, epithelial tissue formation on days 3 and 7, and almost complete bone coverage on day 14 (Fig. 1). The Extraction + BP and Extraction + BP + CY groups showed no changes compared to the Extraction control group immediately after tooth extraction, but food residue was noticeable on day 1 after extraction, and obvious alveolar bone exposure was observed from day 3 after extraction. Epithelialization was gradually observed on day 7, and on day 14, the extraction fossa was almost completely covered with epithelium, as in the Extraction control group. Quantitative evaluation of the open wound area showed no significant differences among the three groups on day 1 after tooth extraction. However, on days 3 and 7,

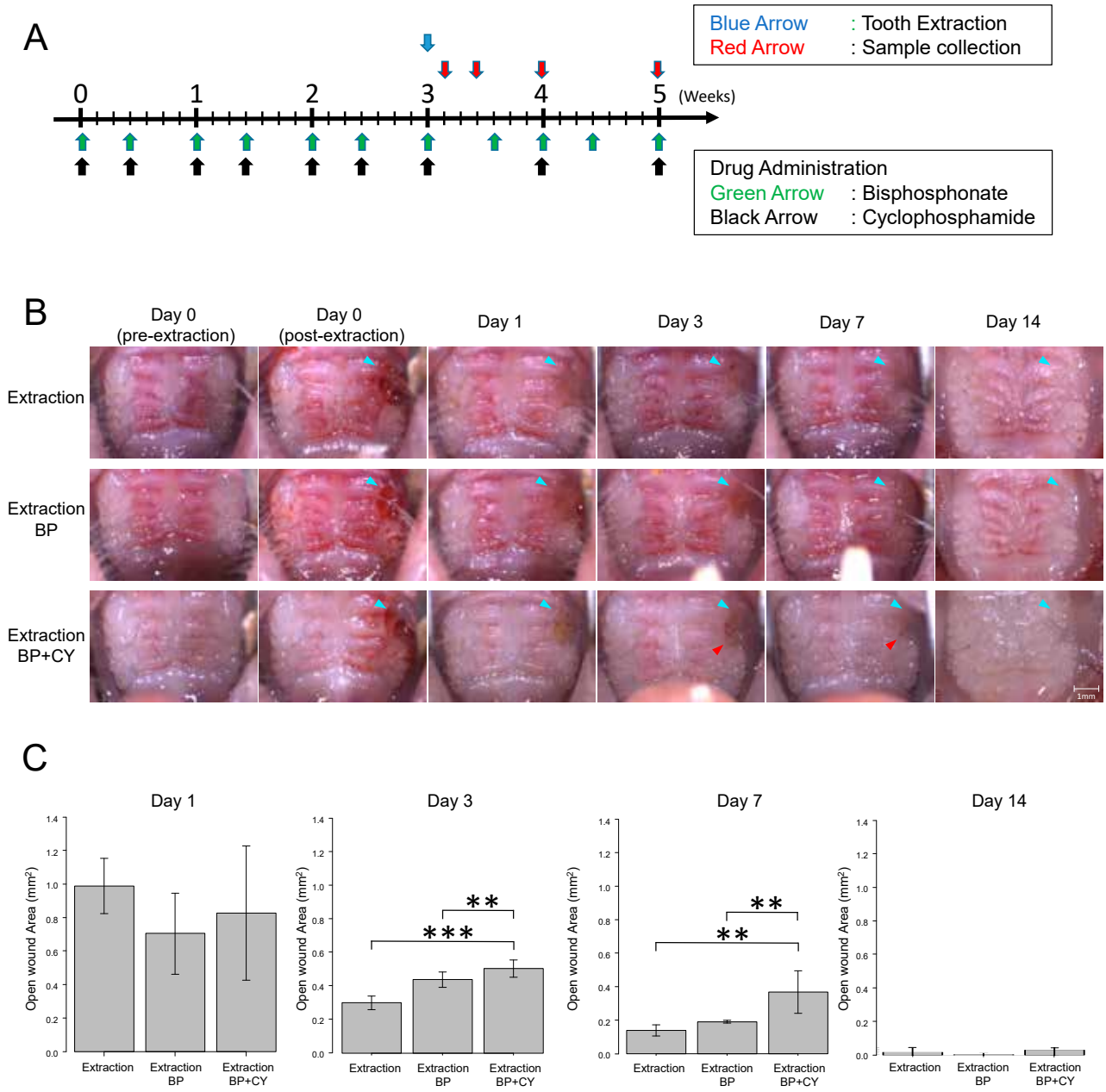

Fig. 1 (A) ARONJ mouse model.
BP (0.05 mg/kg twice a week, s.c.) and/or CY (150 mg/kg twice a week, i.p.) were administered for 3 weeks prior and 2 weeks after tooth extraction.
(B) Representative macroscopic photographs of the experimental site before and after tooth extraction.
Representative macroscopic photographs from three groups (Extraction, Extraction + BP, Extraction + BP + CY) of the tooth extraction site were taken on days 0, 3, 7, and 14 after tooth extraction. Blue arrowheads show tooth extraction site. Red arrowheads show exposed bone. Scale, 1 mm.
(C) Open wound area of tooth extraction site on days 1, 3, 7, and 14 days after tooth extraction. *$P < 0.01$, **$P < 0.001$.

the Extraction + BP and Extraction + BP + CY groups showed significantly larger open wound areas than the Extraction group, indicating delayed healing of the oral mucosa. The open wound area was larger in the Extraction + BP + CY group than in the Extraction + BP group on days 3 and 7, but the differences were not significant. There were no differences in the area of exposed bone among the three groups on day 14 after tooth extraction (Fig. 1C).

Impaired Healing of Extraction Fossa in the ARONJ Model

Next, we examined the effects of drug administration on the alveolar bone after tooth extraction. In micro-CT of horizontal and coronal sections, the Extraction and Extraction + BP groups showed opacities in the extraction fossa suggesting osteoneogenesis (Fig. 2A), while the Extraction + BP + CY group did not. In addition, the Extraction group showed spongy bone permeation in the alveolar bone between the extraction fossae, while the Extraction + BP and Extraction + BP + CY groups showed less spongy bone permeation and osteosclerosis. Quantitative evaluation showed that there was almost no osteoneogenesis in the extraction fossa in the Extraction + BP + CY group. Some osteoneogenesis was observed in the

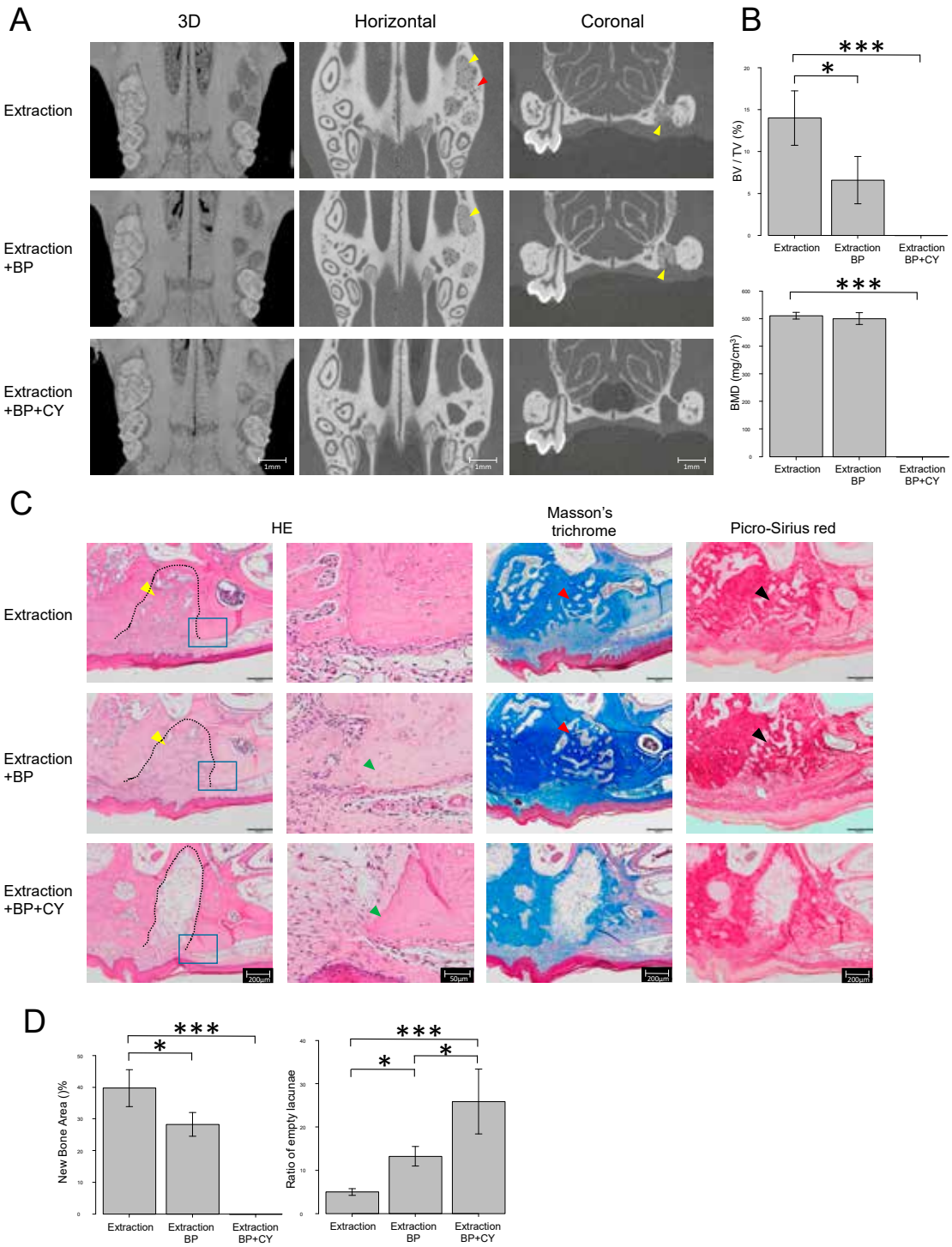

Fig. 2 (A) Micro-CT imaging at tooth extraction site.
Micro-CT images from three groups (Extraction, Extraction + BP, Extraction + BP + CY) for 3D imaging are shown in the left column, with horizontal sections in the middle column and coronal sections in the right column. Micro-CT images were taken on day 7 after tooth extraction. Yellow arrowheads show the new bone in the extraction site, and red arrowheads show the bone marrow cavity-like lesion.
(B) Quantification of bone volume and bone mineral density at the tooth extraction site.
Ratio of new bone volume (BV)/total volume (TV) and bone mineral density (BMD) of tooth extraction site. $*P < 0.05$, $**P < 0.001$.
(C) Histological examination after tooth extraction.
Histological examination was performed on day 7 after tooth extraction. Immunohistochemical images from three groups (Extraction, Extraction + BP, Extraction + BP + CY). H&E staining in the first and second column (images in the left column are higher magnification view of those in the right column), Masson's trichrome staining in the third column, and picro-sirius red staining in the fourth column. Dotted lines show the extraction socket area in alveolar bone. Yellow arrowheads show the new bone in the extraction site. Green arrowheads show the empty lacunae. Red arrowheads show the collagen fiber in the tooth extraction site. Black arrowheads show collagen in the tooth extraction site.
(D) Quantitative evaluation of new bone area and the ratio of empty lacunae.
New bone area (left) and ratio of empty lacunae (right) were quantified in histological sections stained with H&E. $*P < 0.05$, $**P < 0.001$.

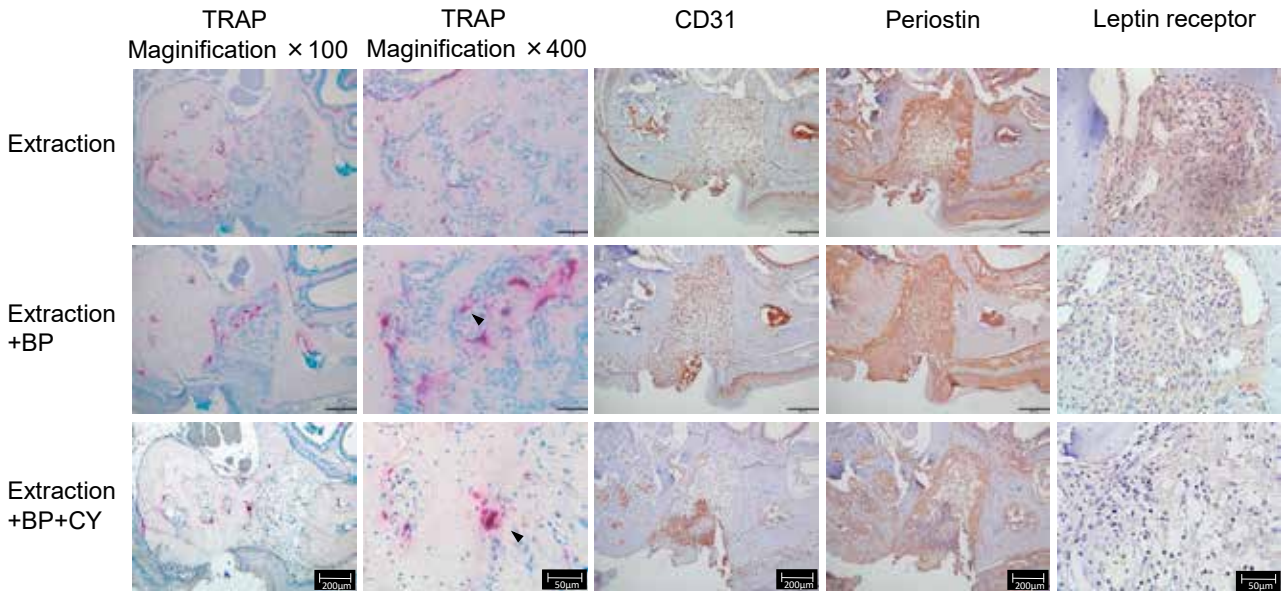

Fig. 3 (A) TRAP staining and immunohistochemistry for CD31, periostin, and leptin receptor at the tooth extraction site. The maxillae harvested on day 7 after tooth extraction were analyzed by TRAP staining, and other histological examinations were performed on maxillae harvested on day 3. TRAP staining and immunohistochemical images from three groups (Extraction, Extraction + BP, Extraction + BP + CY): first column, TRAP staining (×100); second column, TRAP staining (×400); third column, CD31 staining; fourth column, periostin staining; and fifth column, staining for leptin receptor. Black arrowheads show TRAP-positive round multinucleated cells floating around the surface of new bone.

Extraction + BP groups, but it was significantly reduced compared to the Extraction control group. There were no differences in BMD of newly generated bone itself between the Extraction and Extraction + BP groups, indicating that the bone quality was comparable in the two groups (Fig. 2B). The boundary of the extraction fossa was somewhat unclear in H&E-stained sections in both the Extraction and Extraction + BP groups (Fig. 2C), and new bone-like tissue was observed within the extraction fossa. However, in the Extraction + BP + CY group, the extraction fossa boundaries were clear and the root morphology remained intact, with no new bone-like tissue observed. The area of new bone-like tissue in the extraction socket was quantified, and as in micro-CT, almost no new bone was observed in the Extraction + BP + CY group; the levels were significantly lower in the Extraction + BP group than in the control group (Fig. 2D). In the alveolar bone adjacent to the extraction socket, numerous empty lacunae were observed in the Extraction + BP and Extraction + BP + CY groups (Fig. 2C). In quantitative evaluations, the percentage of empty lacunae to all the lacunae in the alveolar bone around the extraction socket was significantly higher in the Extraction + BP and Extraction + BP + CY groups compared to the Extraction control group, and was also predominantly higher in the Extraction + BP + CY group than the Extraction + BP group (Fig. 2D). Masson's trichrome staining showed collagen fibers in the extraction fossa in the Extraction and Extraction + BP groups but not in the Extraction + BP + CY group (Fig. 2C). Continuity of the epithelium directly above the extraction fossa was maintained in all groups. Picro-sirius red staining revealed collagenous tissue in the extraction fossa in the Extraction and Extraction + BP groups but not in the Extraction + BP + CY group. Therefore, it was possible to create an ARONJ-like condition by tooth extraction and administration of BP or BP + CY.

Impaired Cell Mobilization and Angiogenesis in the ARONJ Model

The effects of drug administration on osteoclasts, osteoblast progenitor cells, and blood vessels were examined in the ARONJ model. In TRAP staining, TRAP-positive cells were less obvious in the Extraction + BP + CY group compared to the other groups (Fig. 3). In addition, TRAP-positive cells that did not adhere to the bone surface but rather were detached from it were often observed in the Extraction + BP and Extraction + BP + CY groups (Fig. 3). In immunostaining for CD31, the Extraction + BP + CY group showed fewer CD31-positive cells, especially in the deep part of extraction fossa, although the differences between groups were not obvious (Fig. 3). Periostin immunostaining also showed a trend toward fewer positive cells in the extraction fossa in the Extraction + BP + CY group compared to the other groups, although the differences were not obvious (Fig. 3). Leptin receptor immunostaining showed a large number of positive cells in the extraction fossa in the Extraction group, with fewer in the Extraction + BP and Extraction + BP + CY groups (Fig. 3). These results suggest that both angiogenesis and mobilization of mesenchymal cells (MSCs) and osteoclast progenitor cells were inhibited in the Extraction + BP + CY group.

Angiogenesis in Extraction Socket Healing and its Impairment in the ARONJ Model

During the healing process of the extraction socket, sparse tissue was observed on day 1 after tooth extraction in the Extraction group, but vascular-like structures were observed from day 3, and new bone-like tissue was observed along with vascular-like

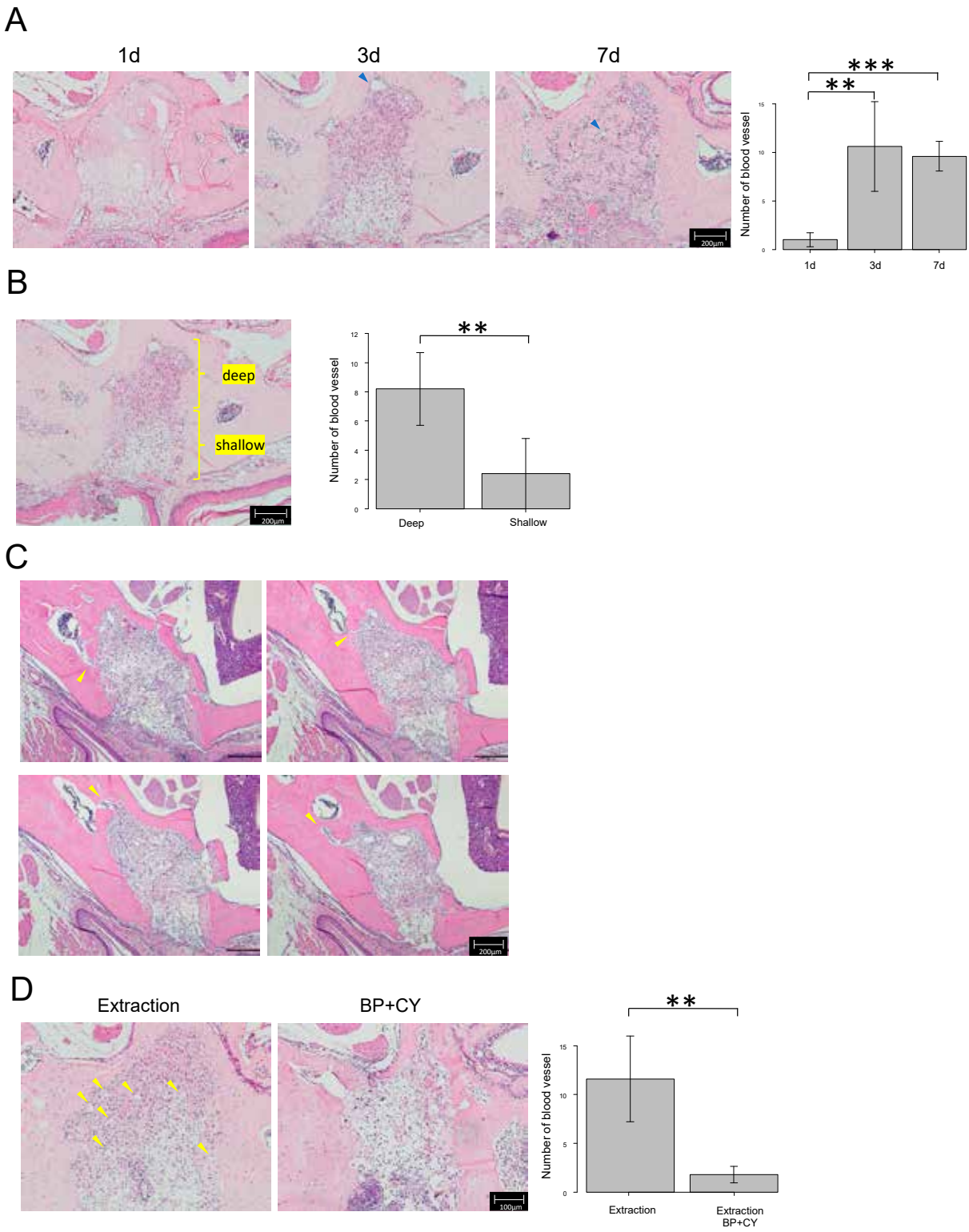

Fig. 4 (A) Representative images of the tooth extraction site with H&E staining on days 1, 3, and 7 after tooth extraction in the Extraction group.
Left: H&E staining of extraction site sections from the Extraction group on days 1, 3, and 7. Red arrowheads show neovasculature and blue arrowhead shows new bone. Right: Quantitative analysis of the blood vessels. *$P < 0.01$, **$P < 0.001$.
(B) Vessel formation and localization after tooth extraction in the Extraction control group.
Histological examination was performed on day 3 after tooth extraction. The tooth extraction area was divided into two regions ("deep" in the bottom of the tooth extraction site and "shallow" in the surface of the tooth extraction site), and the number of vessels in each region was counted. *$P < 0.01$.
(C) Serial sections of H&E staining after tooth extraction in the Extraction control group.
Histological examination was performed on day 3 after tooth extraction. The vasculature was traced to the maxillary bone marrow next to the extraction site in serial sections. Yellow arrowheads show neovasculature connected to the bone marrow.
(D) Representative images of tooth extraction site with H&E staining on day 3 after tooth extraction.
Histological examination was performed on day 3 after tooth extraction. Left: H&E staining of histological section. Right: Quantification of vasculature. *$P < 0.01$.

structures on day 7 (Fig. 4A). The vascular structures were significantly more localized in the deeper than in the shallower parts of the extraction socket (Fig. 4B). The vascular structures were mostly in contact with the surrounding alveolar bone marrow adjacent to the extraction fossa (Fig. 4C). There were significantly fewer such vascular structures in the Extraction + BP + CY group than in the Extraction group (Fig. 4D). These results suggest that drug administration impaired neovascularization to the bone marrow, which may be a reason for the inhibition of cell mobilization suggested by the observations shown in Fig. 3.

Changes in the Bone Marrow of the ARONJ Model

Finally, we examined the number of cells in the adjacent bone marrow, which is assumed to be the source of cells mobilized after tooth extraction. Fig. 5A shows the bone marrow cavity and bone marrow cells adjacent to the tooth extraction socket. There tended to be fewer bone marrow cells in the Extraction + BP + CY group than in the Extraction group. Next, the bone marrow cavity area and the number of cells were quantified. We defined round cells as hematopoietic cells and spindle-shaped cells as MSCs, as described previously [32], and counted the numbers of these cells. There were no significant differences in bone marrow cavity area between groups (Fig. 5B). However, the round cell/area ratio was significantly lower in the Extraction + BP + CY group than in the Extraction group on days 1, 3, and 7 after tooth extraction (Fig. 5C). The spindle cell/area ratio was not significantly different on day 1 after tooth extraction, but was significantly lower in the Extraction + BP + CY group on days 3 and 7 after tooth extraction compared to the Extraction control group, and the difference tended to be smaller than that in the round cell/area ratio (Fig. 5C, D). The spindle cell/round cell ratio was significantly higher in the Extraction + BP + CY group on day 1 after tooth extraction than in the Extraction group, but no differences were observed on days 3 and 7 after tooth extraction (Fig. 5E, F). These results confirmed that the number of cells was also reduced in the bone marrow cavity itself.

DISCUSSION

Several mouse models have been used to analyze the mechanism of ARONJ. BP alone was administered in some studies [18, 33], while many others used BPs in combination with steroids [34] or anticancer drugs [35]. Some protocols adopted various other conditions, such as using ovariectomy-induced osteoporosis [36], immunodeficiency [37], and rheumatoid arthritis [38]. In addition, other environmental factors, such as oral hygiene [39] and the scar healing process [40], are also important for the development of ARONJ. This study was performed using protocols involving the administration of BP alone or in combination with CY. Pharmacologically, BP inhibits osteoclast function via the mevalonic acid pathway, leading to apoptosis [17, 41, 42]. Osteoclasts impaired by BP administration are round in shape and do not attach to the surface of the bone [43], which was also observed in our two experimental groups prepared using BP alone and BP + CY. However, the extents of impairment in the healing of mucosa and bone were more severe in the Extraction + BP + CY group than the Extraction + BP group. As the Extraction + BP + CY group was treated with both antiresorptive therapy and an immune modulator fulfilling the American Association of Oral and Maxillofacial Surgeons (AAOMS) definition of medication-related osteonecrosis of the jaw (MRONJ) [3], it may be more suitable as a model for ARONJ compared to Extraction + BP. MSCs play a major role in wound healing and normal wound healing of extraction fossa, and recovery of ARONJ has been reported following systemic and local administration of MSCs in a mouse model [44, 45]. In this experiment, the leptin receptor expression level, an MSC marker in the skull, tended to be lower in the Extraction + BP and Extraction + BP + CY groups than in the Extraction control group, and the amount of new bone in the extraction fossa was significantly lower in both groups. These observations suggest an association between MSCs and wound healing in the extraction fossa. Cells including MSCs in the wound are generally transported by neovascular vessels. Although the relationship between impairment of angiogenesis and ARONJ has been reported [46], most previous studies regarding ARONJ examined the changes at 2–4 weeks after extraction when the vasculature has already formed. We collected the jawbone within a relatively short time after tooth extraction and examined angiogenesis histologically. In this ARONJ model, histological evaluation revealed that angiogenesis was inhibited as early as 3 days after extraction. To the best of our knowledge, there have been no reports regarding the origin of these new vessels. To determine whether the neovascularization in the extraction fossa originated from the gingival side (periodontal ligament) or the bone marrow, we examined the localization and number of new vessels in the extraction fossa, and found that the vascular structures were predominantly present in the deeper part of the extraction fossa. These observations suggest that there was more neovascularization from the bone marrow than from the gingival side (periodontal ligament). Furthermore, according to the examination of the origin of the neovascularization in serial sections of the same area, traffic was confirmed within the bone marrow and the healing area of the extraction socket in the jawbone. This suggests that there is a close relationship between the neovascular vessels and the bone marrow adjacent to the extraction fossa. Given the suggested relationship between the extraction fossa and the bone marrow, we next evaluated the jaw bone marrow adjacent to the extraction fossa. MSCs are resistant to chemotherapeutic agents, such as methotrexate (MTX) and EN, while hematopoietic cells are not [47]. Hematopoietic cells are generally round, while MSCs are spindle-shaped [32]. Population assessment of cells in the bone marrow near the extraction fossa showed that the Extraction + BP + CY group had a reduced number of bone marrow hematopoietic cells. On the other hand, MSCs tended to be less affected by these drugs than bone marrow hematopoietic cells. MSCs showed no significant difference on day 1 but were significantly decreased on days 3 and 7. This may have been because MSCs are resistant to CY, so their number decreased relatively slowly compared to hematopoietic cells. These results suggest that BP-induced osteonecrosis is localized to the jawbone because the

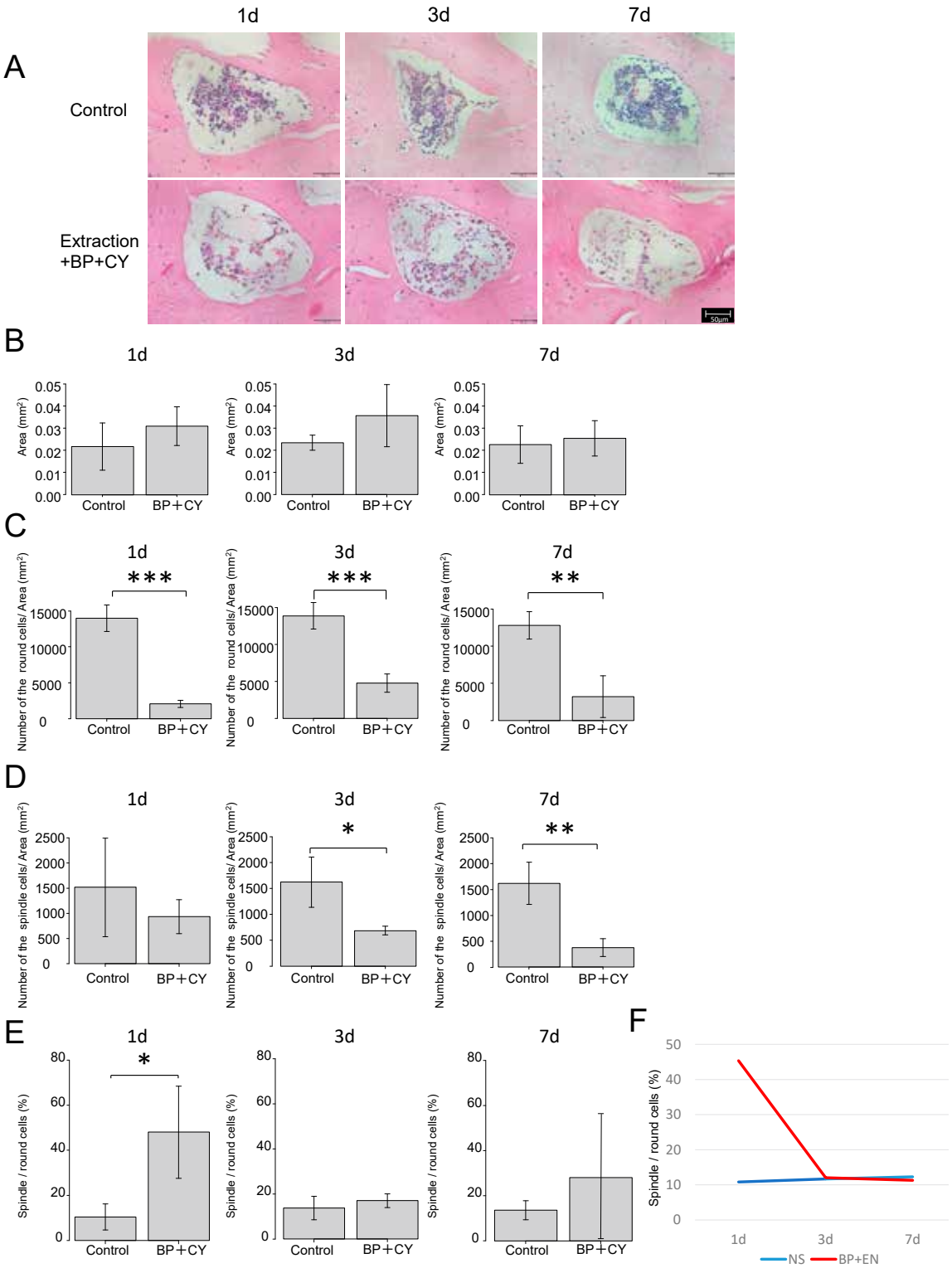

Fig. 5 (A) Representative H&E staining images of maxillary bone marrow close to tooth extraction site.
Representative H&E staining images of maxillary bone marrow close to the tooth extraction site were taken on days 1, 3, and 7 after tooth extraction.
(B) Area of the bone marrow cavity in the extraction site.
Quantification of the area of bone marrow cavities in the Extraction group and Extraction + BP + CY group.
(C) Number of round cells/bone marrow cavity area ratio in the extraction site.
Quantification of the number of round cells bone marrow cavity area ratio for the Extraction group and Extraction + BP + CY group on days 1, 3, and 7 after tooth extraction. $*P < 0.01$, and $**P < 0.001$.
(D) Number of spindle cells/bone marrow cavity area ratio in the extraction site.
Quantification of the number of spindle cells/bone marrow cavity area ratio for the Extraction group and Extraction + BP + CY group on days 3 and 7 after tooth extraction. $*P < 0.05$, $**P < 0.01$.
(E) Number of spindle cells/round cells ratio in the extraction site.
Quantification of the number of spindle cells/round cells ratio for the Extraction group and Extraction + BP + CY group on days 1, 3, and 7 after tooth extraction. $*P < 0.05$.
(F) Time course of changes in spindle cells/round cells ratio in the extraction site.
Plot showing the number of spindle cells/round cells ratio.

wound after tooth extraction is close to the bone marrow, and that local bone marrow MSCs are mobilized into the extraction fossa, whereas circulating bone marrow cells are mobilized into wounds in other extremities. During the healing process of the extraction fossa, angiogenesis occurred in contact with the bone marrow, which was suppressed by drug administration. The number of cells in the bone marrow itself was also reduced by Extraction + BP + CY. Therefore, inhibition of both bone marrow cell mobilization and the angiogenesis necessary for their mobilization may be involved in the pathogenesis of ARONJ.

This study had some limitations. First, this was an *in vivo* study using a mouse model, so further studies are required to determine whether these changes also occur in human ARONJ patients. Second, the period of this study was relatively short (up to 14 days), so further studies to explore the long-term changes induced by the combination of extraction plus BP + CY are required. Third, treatments to induce neovascularization and bone marrow transplantation in these model mice are needed to confirm our hypothesis that both inhibition of angiogenesis and suppression of bone marrow cell mobilization are involved in the pathogenesis of ARONJ.

In conclusion, our results suggest that changes in the bone marrow as well as impairment of neovascularization connecting the bone marrow underlie the pathogenesis of ARONJ. Restoration of jawbone marrow status and vascularization may be useful as a preventive and therapeutic approach for ARONJ.

ACKNOWLEDGMENTS

Financial Support

This work was supported by Japan Society for the Promotion of Science (JSPS) Grant Number 19K10182 (SN), 21H03136(KH). The sponsor or funding organization had no role in the design or conduct of this research.

The authors wish to acknowledge Dr. Yutaka Takazawa, Head of the Pathology Department, Toranomon Hospital, for help in analyzing the condition of bone marrow.

The English in this document has been checked by at least two professional editors, both native speakers of English. For a certificate, please see: http://www.textcheck.com/certificate/VbAUlU

CONFLICT OF INTEREST (COI)

Atsuhiko Hikita held an endowed chair supported by Fujisoft Inc. (until October 31, 2020) and an endowed chair supported by CPC Corp., Kyowa Co., Ltd., Kanto Chemical Co., Inc., and Nichirei Corp. (from July 1, 2021, to June 30, 2022), and is affiliated with the social cooperation program of Kohjin Bio Co., Ltd. (since July 1, 2022).

REFERENCES

1) Marx RE. Pamidronate (Aredia) and zoledronate (Zometa) induced avascular necrosis of the jaws: a growing epidemic. J Oral Maxillofac Surg. 2003 Sep; 61(9): 1115–7.
2) Japanese Allied Committee on Osteonecrosis of the Jaw, Yoneda T, Hagino H, Sugimoto T, Ohta H, Takahashi S, *et al.* Antiresorptive agent-related osteonecrosis of the jaw: Position Paper 2017 of the Japanese Allied Committee on Osteonecrosis of the Jaw. J Bone Miner Metab. 2017 Jan; 35(1): 6–19.
3) Ruggiero SL, Dodson TB, Aghaloo T, Carlson ER, Ward BB, Kademani D. American Association of Oral and Maxillofacial Surgeons' Position Paper on Medication-Related Osteonecrosis of the Jaws-2022 Update. J Oral Maxillofac Surg. 2022 May; 80(5): 920–943.
4) de Cassia Tornier S, Macedo FJ, Sassi LM, Schussel JL. Quality of life in cancer patients with or without medication-related osteonecrosis of the jaw. Support Care Cancer. 2021 Nov; 29(11): 6713–6719.
5) Miksad RA, Lai KC, Dodson TB, Woo SB, Treister NS, Akinyemi O, *et al.* Quality of life implications of bisphosphonate-associated osteonecrosis of the jaw. Oncologist. 2011; 16(1): 121–32. doi: 10.1634/theoncologist. 2010–0183. Epub 2011 Jan 6. PMID: 21212433; PMCID: PMC3228058.
6) Kyrgidis A, Vahtsevanos K, Koloutsos G, Andreadis C, Boukovinas I, Teleioudis Z, *et al.* Bisphosphonate-related osteonecrosis of the jaws: a case-control study of risk factors in breast cancer patients. J Clin Oncol. 2008 Oct 1; 26(28): 4634–8.
7) Vahtsevanos K, Kyrgidis A, Verrou E, Katodritou E, Triaridis S, Andreadis CG, *et al.* Longitudinal cohort study of risk factors in cancer patients of bisphosphonate-related osteonecrosis of the jaw. J Clin Oncol. 2009 Nov 10; 27(32): 5356–62. doi: 10.1200/JCO.2009.21.9584. Epub 2009 Oct 5. PMID: 19805682.
8) Barasch A, Cunha-Cruz J, Curro FA, Hujoel P, Sung AH, Vena D, *et al.* Risk factors for osteonecrosis of the jaws: a case-control study from the CONDOR Dental PBRN. Tex Dent J. 2013 Apr; 130(4): 299–307. PMID: 23767159.
9) Williamson RA. Surgical management of bisphosphonate induced osteonecrosis of the jaws. Int J Oral Maxillofac Surg. 2010 Mar; 39(3): 251–5.
10) Giudice A, Barone S, Diodati F, Antonelli A, Nocini R, Cristofaro MG. Can Surgical Management Improve Resolution of Medication-Related Osteonecrosis of the Jaw at Early Stages? A Prospective Cohort Study. J Oral Maxillofac Surg. 2020 Nov; 78(11): 1986–1999.
11) Gkouveris I, Hadaya D, Elzakra N, Soundia A, Bezouglaia O, Dry SM, *et al.* Inhibition of HMGB1/RAGE Signaling Reduces the Incidence of Medication-Related Osteonecrosis of the Jaw (MRONJ) in Mice. J Bone Miner Res. 2022 Sep; 37(9): 1775–1786.
12) Okawa H, Kondo T, Hokugo A, Cherian P, Sundberg O, Campagna JJ, *et al.* Fluorescent risedronate analogue 800CW-pRIS improves tooth extraction-associated abnormal wound healing in zoledronate-treated mice. Commun Med (Lond). 2022 Sep 5; 2: 112.
13) Rattanawonsakul K, Bullock G, Bolt R, Claeyssens F, Atkins S, Hearnden V. In vitro Effect of Geranylgeraniol (GGOH) on Bisphosphonate-Induced Cytotoxicity of Oral Mucosa Cells. Front Oral Health. 2022 Jun 20; 3: 892615.
14) Chin KY, Ekeuku SO, Trias A. The Role of Geranylgeraniol in Managing Bisphosphonate-Related Osteonecrosis of the Jaw. Front Pharmacol. 2022 May 4; 13: 878556.
15) Zhao D, Xiao D, Liu M, Li J, Peng S, He Q, *et al.* Tetrahedral framework nucleic acid carrying angiogenic peptide prevents bisphosphonate-related osteonecrosis of the jaw by promoting angiogenesis. Int J Oral Sci. 2022 Apr 27; 14(1): 23.
16) Freiberger JJ. Utility of hyperbaric oxygen in treatment of bisphosphonate-related osteonecrosis of the jaws. J Oral Maxillofac Surg. 2009 May; 67(5 Suppl): 96–106.
17) Cremers S, Drake MT, Ebetino FH, Bilezikian JP, Russell RGG. Pharmacology of bisphosphonates. Br J Clin Pharmacol. 2019 Jun; 85(6): 1052–1062.
18) Zhu W, Xu R, Du J, Fu Y, Li S, Zhang P, *et al.* Zoledronic acid promotes TLR-4-mediated M1 macrophage polarization in bisphosphonate-related osteonecrosis of the jaw. FASEB J. 2019 Apr; 33(4): 5208–5219.
19) Qu X, Sun Z, Wang Y, Ong HS. Zoledronic acid promotes osteoclasts ferroptosis by inhibiting FBXO9-mediated p53 ubiquitination and degradation. PeerJ. 2021 Dec 16; 9: e12510.
20) Yang G, Singh S, McDonough CW, Lamba JK, Hamadeh I, Holliday LS, *et al.* Genome-wide Association Study Identified Chromosome 8 Locus Associated with Medication-Related Osteonecrosis of the Jaw. Clin Pharmacol Ther. 2021 Dec; 110(6): 1558–1569.

21) Reid IR, Cornish J. Epidemiology and pathogenesis of osteonecrosis of the jaw. Nat Rev Rheumatol. 2011 Nov 29; 8(2): 90–6.
22) Hamadeh IS, Ngwa BA, Gong Y. Drug induced osteonecrosis of the jaw. Cancer Treat Rev. 2015 May; 41(5): 455–64.
23) Gkouveris I, Hadaya D, Soundia A, Bezouglaia O, Chau Y, Dry SM, *et al*. Vasculature submucosal changes at early stages of osteonecrosis of the jaw (ONJ). Bone. 2019 Jun; 123: 234–245.
24) Yi Y, Stenberg W, Luo W, Feng JQ, Zhao H. Alveolar Bone Marrow Glil + Stem Cells Support Implant Osseointegration. J Dent Res. 2022 Jan; 101(1): 73–82. doi: 10.1177/00220345211013722. Epub 2021 May 19. PMID: 34009063; PMCID: PMC8721727.
25) Ito K, Muraoka H, Hirahara N, Sawada E, Hirohata S, Otsuka K, *et al*. Quantitative assessment of mandibular bone marrow using computed tomography texture analysis for detect stage 0 medication-related osteonecrosis of the jaw. Eur J Radiol. 2021 Dec; 145: 110030.
26) Muraoka H, Ito K, Hirahara N, Okada S, Kondo T, Kaneda T. The value of diffusion-weighted imaging in the diagnosis of medication-related osteonecrosis of the jaws. Oral Surg Oral Med Oral Pathol Oral Radiol. 2021 Sep; 132(3): 339–345.
27) Kuroshima S, Sasaki M, Nakajima K, Tamaki S, Hayano H, Sawase T. Prevalence of bisphosphonate-related osteonecrosis of the jaw-like lesions is increased in a chemotherapeutic dose-dependent manner in mice. Bone. 2018 Jul; 112: 177–186.
28) Kozutsumi R, Kuroshima S, Kaneko H, Sasaki M, Ishisaki A, Sawase T. Zoledronic Acid Deteriorates Soft and Hard Tissue Healing of Murine Tooth Extraction Sockets in a Dose-Dependent Manner. Calcif Tissue Int. 2022 Jan; 110(1): 104–116.
29) Kawai S, Takagi Y, Kaneko S, Kurosawa T. Effect of three types of mixed anesthetic agents alternate to ketamine in mice. Exp Anim. 2011; 60(5): 481–7.
30) Schneider CA, Rasband WS, Eliceiri KW. NIH Image to ImageJ: 25 years of image analysis. Nat Methods. 2012 Jul; 9(7): 671–5.
31) Kanda Y. Investigation of the freely available easy-to-use software 'EZR' for medical statistics. Bone Marrow Transplant. 2013 Mar; 48(3): 452–8.
32) Roubelakis MG, Tsaknakis G, Pappa KI, Anagnou NP, Watt SM. Spindle shaped human mesenchymal stem/stromal cells from amniotic fluid promote neovascularization. PLoS One. 2013; 8(1): e54747.
33) Rao NJ, Wang JY, Yu RQ, Leung YY, Zheng LW. Role of Periapical Diseases in Medication-Related Osteonecrosis of the Jaws. Biomed Res Int. 2017; 2017: 1560175.
34) Sonis ST, Watkins BA, Lyng GD, Lerman MA, Anderson KC. Bony changes in the jaws of rats treated with zoledronic acid and dexamethasone before dental extractions mimic bisphosphonate-related osteonecrosis in cancer patients. Oral Oncol. 2009 Feb; 45(2): 164–72.
35) Tanaka Y, Aung KT, Ono M, Mikai A, Dang AT, Hara ES, *et al*. Suppression of Bone Necrosis around Tooth Extraction Socket in a MRONJ-like Mouse Model by E-rhBMP-2 Containing Artificial Bone Graft Administration. Int J Mol Sci. 2021 Nov 26; 22(23): 12823.
36) Kim JW, Tatad JCI, Landayan MEA, Kim SJ, Kim MR. Animal model for medication-related osteonecrosis of the jaw with precedent metabolic bone disease. Bone. 2015 Dec; 81: 442–448.
37) Rao NJ, Yu RQ, Wang JY, Helm A, Zheng LW. Effect of Periapical Diseases in Development of MRONJ in Immunocompromised Mouse Model. Biomed Res Int. 2019 Sep 22; 2019: 1271492. doi: 10.1155/2019/1271492. PMID: 31662968; PMCID: PMC6778953.
38) de Molon RS, Hsu C, Bezouglaia O, Dry SM, Pirih FQ, Soundia A, *et al*. Rheumatoid Arthritis Exacerbates the Severity of Osteonecrosis of the Jaws (ONJ) in Mice. A Randomized, Prospective, Controlled Animal Study. J Bone Miner Res. 2016 Aug; 31(8): 1596–607.
39) Castillo EJ, Messer JG, Abraham AM, Jiron JM, Alekseyenko AV, Israel R, *et al*. Preventing or controlling periodontitis reduces the occurrence of osteonecrosis of the jaw (ONJ) in rice rats (Oryzomys palustris). Bone. 2021 Apr; 145: 115866.
40) Vieira AE, Repeke CE, Ferreira Junior Sde B, Colavite PM, Biguetti CC, Oliveira RC, *et al*. Intramembranous bone healing process subsequent to tooth extraction in mice: micro-computed tomography, histomorphometric and molecular characterization. PLoS One. 2015 May 29; 10(5): e0128021.
41) Fisher JE, Rodan GA, Reszka AA. In vivo effects of bisphosphonates on the osteoclast mevalonate pathway. Endocrinology. 2000 Dec; 141(12): 4793–6.
42) Frith JC, Mönkkönen J, Auriola S, Mönkkönen H, Rogers MJ. The molecular mechanism of action of the antiresorptive and antiinflammatory drug clodronate: evidence for the formation in vivo of a metabolite that inhibits bone resorption and causes osteoclast and macrophage apoptosis. Arthritis Rheum. 2001 Sep; 44(9): 2201–10.
43) Sakai H, Kobayashi Y, Sakai E, Shibata M, Kato Y. Cell adhesion is a prerequisite for osteoclast survival. Biochem Biophys Res Commun. 2000 Apr 13; 270(2): 550–6.
44) Kikuiri T, Kim I, Yamaza T, Akiyama K, Zhang Q, Li Y, *et al*. Cell-based immunotherapy with mesenchymal stem cells cures bisphosphonate-related osteonecrosis of the jaw-like disease in mice. J Bone Miner Res. 2010 Jul; 25(7): 1668–79. doi: 10.1002/jbmr.37. PMID: 20200952; PMCID: PMC3154005.
45) Barba-Recreo P, Del Castillo Pardo de Vera JL, Georgiev-Hristov T, Ruiz Bravo-Burguillos E, Abarrategi A, Burgueño M, *et al*. Adipose-derived stem cells and platelet-rich plasma for preventive treatment of bisphosphonate-related osteonecrosis of the jaw in a murine model. J Craniomaxillofac Surg. 2015 Sep; 43(7): 1161–8.
46) Sharma D, Ivanovski S, Slevin M, Hamlet S, Pop TS, Brinzaniuc K, *et al*. Bisphosphonate-related osteonecrosis of jaw (BRONJ): diagnostic criteria and possible pathogenic mechanisms of an unexpected anti-angiogenic side effect. Vasc Cell. 2013 Jan 14; 5(1): 1.
47) Li J, Law HK, Lau YL, Chan GC. Differential damage and recovery of human mesenchymal stem cells after exposure to chemotherapeutic agents. Br J Haematol. 2004 Nov; 127(3): 326–34.